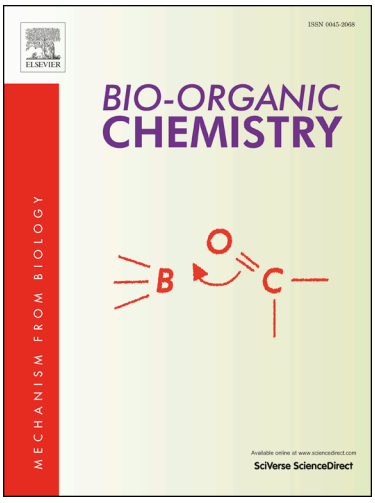

Synthesis and biological evaluation of *N*-aryl-2-phenyl-hydrazinecarbothioamides: Experimental and theoretical analysis on tyrosinase inhibition and interaction with HSA

Danilo Sousa-Pereira, Otávio Augusto Chaves, Camilla Moretto dos Reis, Márcia C. C. de Oliveira, Carlos Maurício R. Sant'Anna, José Carlos Netto-Ferreira, Aurea Echevarria

PII: S0045-2068(18)30370-5
DOI: https://doi.org/10.1016/j.bioorg.2018.07.035
Reference: YBIOO 2454

To appear in: *Bioorganic Chemistry*

Received Date: 17 April 2018
Revised Date: 20 July 2018
Accepted Date: 31 July 2018

Please cite this article as: D. Sousa-Pereira, O. Augusto Chaves, C. Moretto dos Reis, M. C. C. de Oliveira, C. Maurício R. Sant'Anna, J. Carlos Netto-Ferreira, A. Echevarria, Synthesis and biological evaluation of *N*-aryl-2-phenyl-hydrazinecarbothioamides: Experimental and theoretical analysis on tyrosinase inhibition and interaction with HSA, *Bioorganic Chemistry* (2018), doi: https://doi.org/10.1016/j.bioorg.2018.07.035

Synthesis and biological evaluation of *N*-aryl-2-phenyl-hydrazinecarbothioamides: Experimental and theoretical analysis on tyrosinase inhibition and interaction with HSA

Danilo Sousa-Pereira,[a,†] Otávio Augusto Chaves,[a,†] Camilla Moretto dos Reis,[a] Márcia C. C. de Oliveira,[a] Carlos Maurício R. Sant'Anna,[a] José Carlos Netto-Ferreira,[a,b,*] Aurea Echevarria,[a,*]

[a]Departmento de Química, Universidade Federal Rural do Rio de Janeiro-UFRRJ, 23851-970, Seropédica-RJ, Brazil.

[b]Instituto Nacional de Metrologia, Qualidade e Tecnologia-INMETRO, Divisão de Metrologia Química, 25250-020, Duque de Caxias-RJ, Brazil.

† These authors contributed equally to this work

*Corresponding authors: jcnetto@ufrrj.br (**J. C. Netto-Ferreira**) and echevarr@ufrrj.br(**A. Echevarria**).

Abstract

A series of *N*-aryl-2-phenyl-hydrazinecarbothioamides have been investigated as possible inhibitors of tyrosinase, an enzyme involved in the development of melanomas. The hydrazinecarbothioamides **1**-**6** were synthesized from the reaction between phenylhydrazine and isothiocyanates, for which three different methods have been employed, namely stirring at room temperature, by microwave irradiation or by mechanochemical grinding. Quantitative yields were obtained for the later technique. Compound **4** showed the best valuefortyrosinase inhibition (IC_{50} = 22.6 μM), which occurs through an uncompetitive mechanism. Molecular docking results suggested that **4** can interact *viaT*-stacking with the substrate L-DOPA and *via* hydrogen bonding and hydrophobic forces with the amino acid residues Ala-79, His-243, Val-247, Phe-263, Val-282, and Glu-321. The interaction between human serum albumin (HSA) and compound **4** occurs through a ground state association and does not perturb the secondary structure of the albumin as well as the microenvironment around Tyr and Trp residues. The binding is spontaneous, moderate and occurs mainly in the Sudlow's site I. Molecular docking results suggested hydrogen bonding, hydrophobic and electrostatic interactions as the main binding forces between the compound **4** and the amino acid residues Lys-198, Trp-214, Glu-449, Leu-452, and Leu-480.

Keywords:*N*-aryl-2-phenyl-hydrazinecarbothioamides; mechanochemical grinding; enzyme tyrosinase; human serum albumin; spectroscopy; molecular docking.

1. Introduction

Enzyme tyrosinase (EC 1.14.18.1), also known as polyphenol oxidase (PPO), is a copper-containing enzyme widely distributed in fungi, plants, and animals. It can catalyze the skin pigmentation and is directly related to pigmentation disorders in mammals [1]. Tyrosinase activity is related to its ability to catalyze the aerobic hydroxylation of L-tyrosine to L-DOPA and the subsequent oxidation of the later to L-Dopaquinone, which leads to melanin accumulation and hyper pigmentation [2]. Recently, it has been demonstrated that various dermatological disorders, such as age spots, melasma freckle, and sites of actinic damage can be caused by the accumulation of an excessive level of epidermal pigmentation and not only by ultraviolet radiation. Thus, the inhibitory action on tyrosinase activity minimizes the occurrence of dermatological disorders, mainly melanomas, becoming the major target in the treatment of disorders related to the abnormal accumulation of melanin [2,3].

Carbothioamide derivatives were already tested as tyrosinase inhibitors, among them a series of 1-(1-arylethylidene) thiosemicarbazide with the derivatives containing either a 4-methoxyphenyl or a 2-thiophenyl group showed IC_{50} = 0.11 µM and 0.14 µM, respectively [4]. Besides 1-(1-(4-methoxyphenyl)-3-phenylallylidene) thiosemicarbazide exhibited IC_{50} = 0.27 µM [5] and 4-methyl-1-(2-(4-methyl-2-oxo-2*H*-chromen-7-yloxy)acetyl) thiosemicarbazide IC_{50} = 10.5 µM [6]. Recently, the (*Z*)-2-(3-(phenethylamino)-but-2-enoyl)-hydrazine-carbothioamide showed potential tyrosinase inhibition (89%) through an uncompetitive inhibitory mechanism and IC_{50} = 49 µM [3].

Human serum albumin (HSA) is the major protein in human bloodstream and accounts for almost 60% of total plasma protein content. Serum albumin functional activity is essential for maintaining normal tissue and organ homeostasis, but its function depends on

both its concentration and structure. HSA is the main transporting protein for ligands due to its ability to bind to a broad range of both hydrophobic and hydrophilic molecules, including drugs [7,8]. HSA has a molecular weight of 66.7 kDa and is composed of a single polypeptide chain containing 585 amino acids,among them one tryptophan residue (Trp-214), seventeen tyrosine residues (Tyr-30, -84, -138, -140, -148, -150, -161, -263, -319, -332, -334, -341, -353, -370, -401, -411, -497), a free thiol group of a cysteine residue (Cys-34) and seventeen intramolecular disulfide bridges [9,10].

In the present work six hydrazinecarbothioamides (Fig. 1),*i. eN*-2-diphenylhydrazinecarbothioamide (**1**); *N*-(4-nitrophenyl)-2-phenylhydrazinecarbothioamide (**2**); *N*-(4-chlorophenyl)-2-phenylhydrazinecarbothioamide (**3**); *N*-(4-bromophenyl)-2-phenylhydrazinecarbothioamide (**4**); *N*-(4-methoxyphenyl)-2-phenylhydrazinecarbothioamide (**5**) and *N*-(*p*-tolyl)-2-phenyl-hydrazinecarbothioamide (**6**) were synthesized and characterized. The experimental and theoretical evaluation of the action of these compounds as tyrosinase inhibitors was then performed. In addition, as the distribution and metabolism of many biologically active compounds in the body are correlated to their affinity for serum albumin, the interaction between the most potential tyrosinase inhibitor,*i.e.***4**, and HSA was investigated under physiological conditions by multiple spectroscopic techniques (circular dichroism, steady-state, time-resolved and synchronous fluorescence) combined with molecular docking.

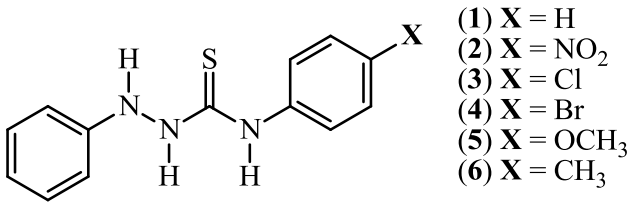

Fig. 1. Chemical structure for the *N*-aryl-2-phenyl-hydrazinecarbothioamides **1-6**.

2. Results and Discussion

2.1. *N*-aryl-2-phenyl-hydrazinecarbothioamides synthesis

N-aryl-2-phenyl-hydrazinecarbothiamides **1-6** were obtained by an anhydrous acylation reaction between phenylhydrazine and 4-X-phenyl-isothiocyanates employing initially two very well knownsynthetic methods for these type of compounds: (I) stirring in hot toluene for 60 min, and (II) under microwave irradiation for 30 min [11]. Further, mechanochemistry [12] was used as a novel method (method III, in Scheme 1) for the synthesis of hydrazinecarbothiamides, in which phenylhydrazine was milled in the presence of 4-X-phenyl-isothiocyanates in a porcelain mortar under solvent-free conditions, at room temperature, during a very short reaction time (2 min) (Scheme 1).

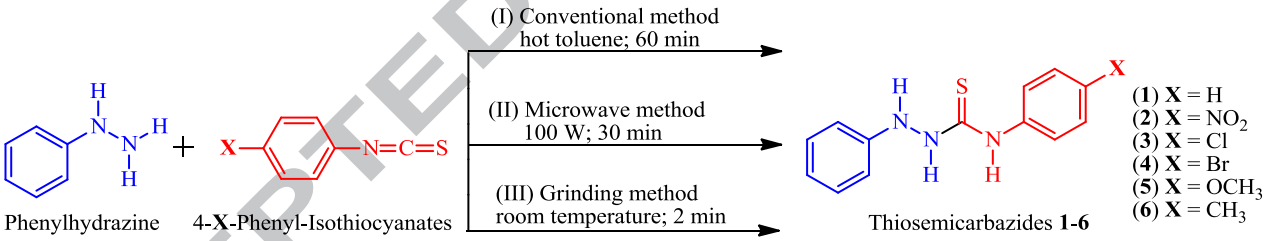

Scheme 1. Thesynthetic route for the preparation of compounds **1-6**.

Reaction products were obtained in quantitative yields and high-purity using method III when compared to the traditional procedure (I, 60 min, 68-95%) or to microwave irradiation (II, 30 min, 66-83%). Method III allowed the synthesis of the target compounds in solvent-free conditions and high purity, without the need for further recrystallization.

The methods II and III were aimed to obtain a reduction in the reaction time as well as to fulfill some of the principles of Green Chemistry [13]. However, the

hydrazinecarbothiamidespreparation *via* the traditional methodology using toluene as the solvent and under stirring at room temperature (I) was more efficient than the microwave-assisted procedure (II), affording better yields on the formation of products. This result may be due to the high volatility of the isothiocyanates employed as starting materials. Table 1 shows the product yields obtained in the preparation of **1-6**. The hydrazinecarbothiamides were fully characterized by ^{1}H- and DEPT Q-NMR and IR spectroscopy, and identified by comparison with spectroscopic data from the literature (Fig. 1S-6S in the supplementary material) [14,15]. The chemical shift values for H-1 (δ7.38 to 7.53, Δ = 0.15) did not show significant differences as a function of the different substituents on the N-4 linked ring. However, the chemical shift values for H-2 and H-4 showed range of δ9.51 to 10.19 (Δ = 0.51) and δ8.60 to 9.08 (Δ = 0.48), respectively, due the deshielding effects of withdraw moieties NO_2, Cl and Br, when compared to the presence of donor electron groups OCH_3 and CH_3.

Table 1

Yields and corresponding melting points(ºC) for the thiosemicarbazides **1-6**obtained under methods I or II.

Thiosemicarbazides	**X**	Yield (%) / Method		mp(ºC)
		Conventional Method (I; 60 min)	Microwave Irradiation (II; 30 min)	
1	H	92	83	171-173
2	NO_2	95	73	233-234
3	Cl	68	66	233-234
4	Br	93	80	209-212
5	OCH_3	92	80	184-186
6	CH_3	92	78	174-175

2.2. Tyrosinase inhibitory assay. Experimental and theoretical approach

A preliminary screening employing colorimetric assays with the enzyme tyrosinase showed that hydrazinecarbothiamides**1-6** were able to inhibit the oxidation of L-DOPA, the

substrate for the diphenolase activity of mushroom tyrosinase, with inhibition percentage of 73%; 81%; 98%; 96%; 17% and 29% for hydrazinecarbothiamides**1**, **2**, **3**, **4**, **5** and **6**, respectively. The IC_{50} values obtained for the more active compounds, *i. e.***1**, **2**, **3** and **4** are in the order of 623.00; 189.00; 56.50 and 22.60 μM, respectively(Fig. 7S in the supplementary material). Overall, the hydrazinecarbothiamides substituted with an electron acceptor group showed better tyrosinase inhibition than the commercial standard ascorbic acid (IC_{50} = 266.00μM) [3]. In addition, hydrazinecarbothiamides**4** showed the best inhibitory effect among all compounds analyzed.

The inhibitory mechanism in the mushroom tyrosinase, as well as the kinetic parameters associated to it, were determined in the presence of the two best inhibitors of tyrosinase, **3** and **4**, employing Hanes-Woof plots (Fig. 2 and Table 2). Since K_m(Michaelis-Menten constant) andV_m(maximum velocity in the presence of each inhibitor) in the absence of the hydrazinecarbothiamides**3** and **4** showed higher values than those in the presence of these two inhibitors, at different concentrations, it can be concluded that the mechanism of inhibition of tyrosinase by**3** and **4**is uncompetitive [3]. Thus, the potential inhibitors bind reversibly to the enzyme-substrate (ES) complex, providing a ternary complex enzyme-substrate-inhibitor (ESI). This result indicates that thehydrazinecarbothiamides**3** and **4** do not bind to the free enzyme, which allows an increase in the degree of inhibition as the concentration of the substrate increases in the reaction medium.

Table 2

Kinetic parameters (K_m and V_m) for the tyrosinase activity in the absence and in the presence of different concentrations of hydrazinecarbothiamides**3** or **4** (0.00; 83.0; 50.0 and 33.3 μM).

Kinetic parameters	Without**3**or**4**	**3**or**4** (83.0 μM)	**3**or**4** (50.0 μM)	**3**or**4** (33.3 μM)
K_m(μM)	(3.00 or 2.79) $x10^{-3}$	(2.13 or 1.23) $x10^{-2}$	(2.11 or 2.24) $x10^{-2}$	(1.35 or 2.22) $x10^{-2}$
V_m(μM/min)	20.8 or 22.10	11.8 or 9.72	13.1or 7.28	20.1or 8.67

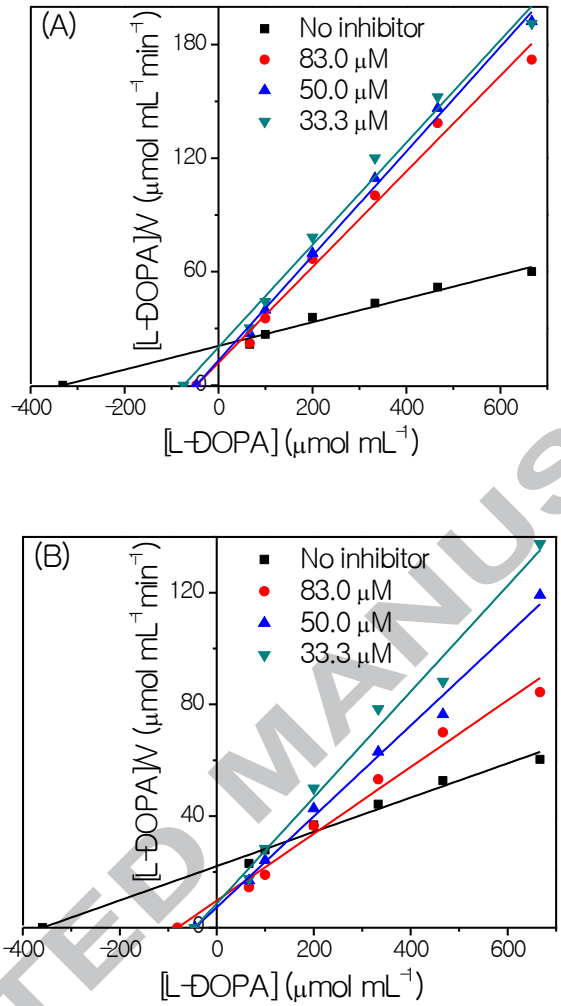

Fig. 2. Hanes-Woof plots for tyrosinase in the presence of L-DOPA and hydrazinecarbothiamide**3** (A) and **4** (B). [L-DOPA] = 66.6; 100; 200; 333; 467 and 667 μM and [**3**] = [**4**] = 0.00; 33.3; 50.0 and 83.0 μM.

In order topropose a molecular level explanation on the tyrosinase inhibition by the four best inhibitors (hydrazinecarbothiamides derivatives **1-4**), a molecular docking study was carried out assuming the ESI complex formation (uncompetitive inhibitory mechanism). In this case, due to interaction between one of the phenolic hydroxyl group from the L-DOPA structure (substrate) with Cu^{2+}, the acidity of this group has increased and the molecular docking calculations assumed a deprotonation state. Fig. 3 depicts the best docking pose for all hydrazinecarbothiamides under study in the presence of L-DOPA. As expected, in the

presence of the substrate molecule the electron donor group present in the hydrazinecarbothiamide structure is not near enough to coordinate with the dicopper center, suggesting that the tyrosinase inhibition by **1-4** is not related to the Cu^{2+} coordination ability. In fact, one of the hydroxyl groups belonging to L-DOPA is near enough to coordinate with the dicopper center, within a distance of 2.30 Å. The molecular docking results for the best pose inside the protein pocket (Fig. 3A) suggest that the interactionsof **3** and **4**with the active site are essentially of a hydrophobic nature, involving *T*-stacking with the aromatic ring of L-DOPA. On the other hand, inhibitors **1** and **2**do not show significant intermolecular interaction with this substrate. Thus, the low IC_{50} value for hydrazinecarbothiamides**1** and **2** could probably be related to its low affinity for the substrate L-DOPA, while **3** and **4** presented similar IC_{50} values due to their high ability for this substrate.

Fig. 3B shows the main amino acid residues that interact with the two best experimental tyrosinase inhibitors, *i. e*hydrazinecarbothiamides**3** and **4,** which are superimposed on the figure for a comparison of their interaction profiles. Despite the fact that the ligands can interact *via**T*-stacking with L-DOPA, one N-H group of the ligandsisa potential hydrogen bond donor with the amino acid residue Glu-321, within an intermolecular interaction distance of 2.73 Å. Molecular docking results also suggested hydrophobic interactions between the structure of the ligands and Ala-79, His-243, Val-247, Phe-263, and Val-282residues.

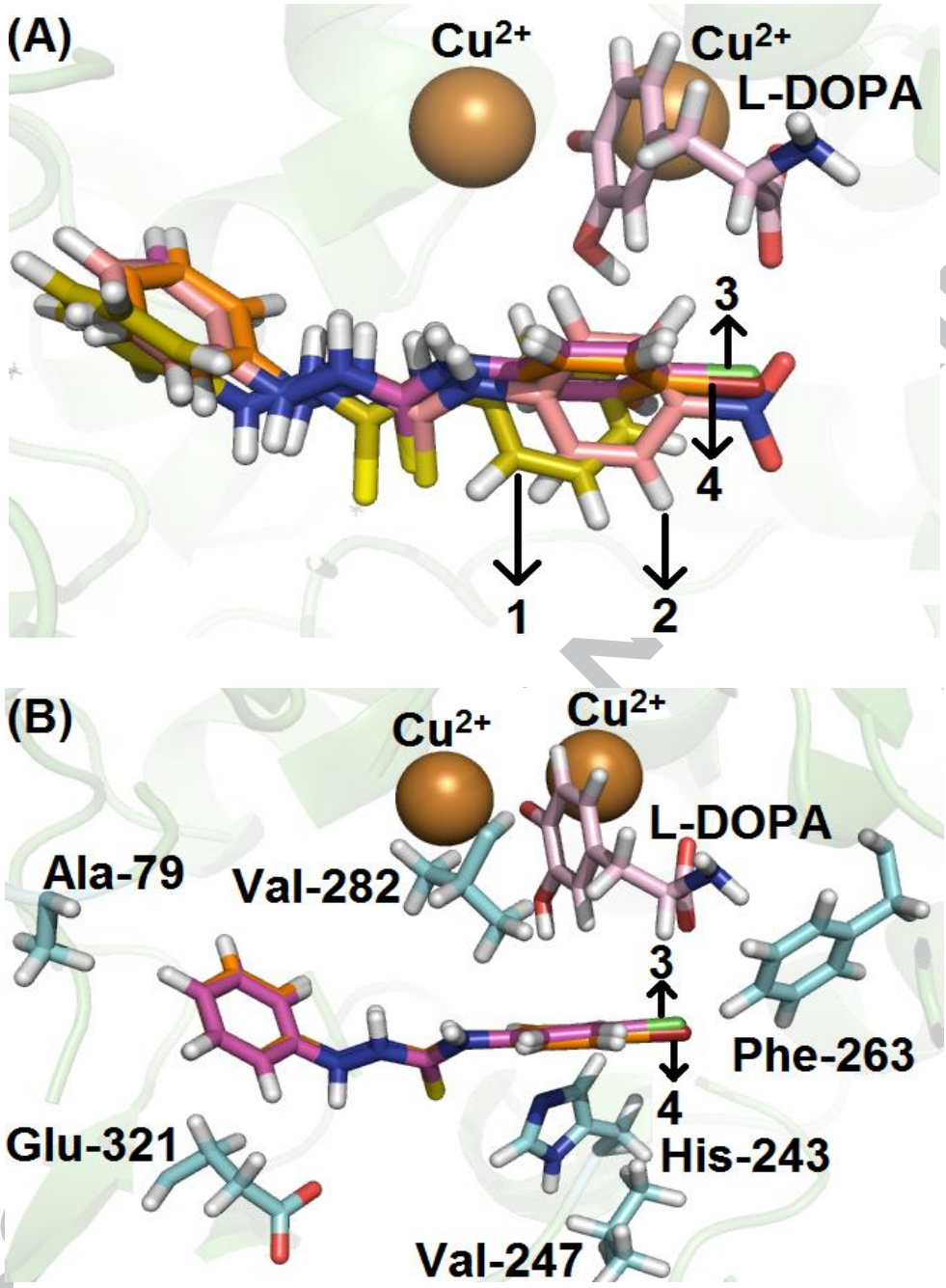

Fig. 3. (A) Superposition of the best docking poses for the interaction between tyrosinase and hydrazinecarbothiamides**1-4** in the presence of L-DOPA (*GoldScore* function). (B) Superposition between hydrazinecarbothiamides**3** and **4** and representation of the main amino acid residues which interact with these inhibitors. Tyrosinase is in green cartoon representation; L-DOPA and selected amino acid residues are represented in violet and cyan, respectively. Hydrazinecarbothiamides**1-4** are represented in olive, salmon, magenta, and orange, respectively. Copper atoms are represented as brown spheres. Black dots represent interaction *via* hydrogen bonding. Element colors: hydrogen: white; oxygen: red; nitrogen: dark blue; bromine: brownish red, chloro: dark green and sulfur: yellow.

2.3. HSA binding studies

2.3.1. Interaction between HSA and the hydrazinecarbothiamide 4

Steady-state fluorescence quenching is considered as an effective approach to investigate the transport ability of HSA towards small molecules [16]. Fig. 4 depicts the fluorescence emission of HSA and its quenching upon successive additions of the best tyrosinase inhibitor under study (compound **4**), at 310 K. Fluorescence quenching occurs in the presence of **4** and there is no significant change in the position of the maximum emission for HSA (λ_{em} = 340 nm) upon ligand binding. This is a clear indication that the ligand is able to bind near the Trp-214 residue and that it does not perturb the microenvironment surrounding this residue [8].

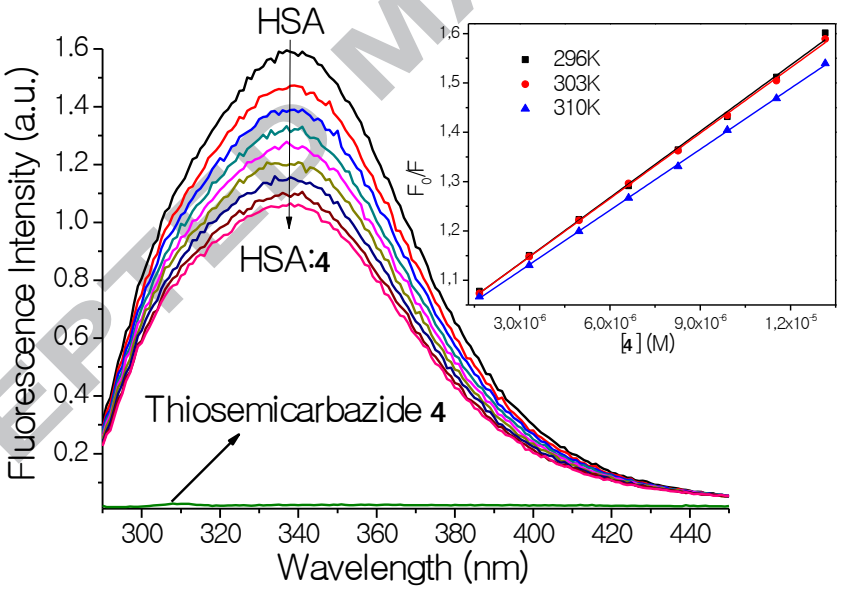

Fig. 4. Steady-state fluorescence emission of hydrazinecarbothiamide**4** and HSA without and in the presence of successive additions of **4** at pH 7.4 and 310 K. *Inset*: Stern-Volmer plots for the interaction HSA:**4** at 296 K, 303 K and 310 K. [HSA] = 1.0 x 10^{-5} M and [**4**] = 0.17; 0.33; 0.50; 0.66; 0.83; 0.99; 1.15; and 1.32 x 10^{-5} M.

Steady-state fluorescence quenching may be due to a dynamic and/or static mechanism and a Stern-Volmer analysis can be used to identify which fluorescence mechanism must be occurring (Eq. 1) [17]:

$$\frac{F_0}{F} = 1 + k_q \tau_0 [Q] = 1 + K_{SV}[Q] \quad (1)$$

where F_0 and F are the steady-state fluorescence intensities of HSA in the absence and presence of **4** at 340 nm, respectively. [*Q*] is the quencher concentration, K_{SV} and k_q are the Stern-Volmer constant and the bimolecular quenching rate constant, respectively. τ_0 is the HSA fluorescence lifetime in the absence of quenchers. The experimental average value measured in this work for the fluorescence lifetime of HSA in PBS was (5.75±0.10) x 10^{-9} s.

Table 3 shows the K_{SV} and k_q values for the interaction HSA:**4** at 296 K, 303 K, and 310 K. Since the K_{SV} values decrease with the increase of the temperature and the k_q values are higher than the limiting diffusion rate constant in water (k_{diff} ≈7.40 × 10^9 $M^{-1}s^{-1}$, according to Smoluchowski-Stokes-Einstein theory at 298 K) [18],the main fluorescence quenching mechanism must be static, which indicates that a ground state association between HSA and **4**must be present [19].

Time-resolved fluorescence is a sensitive technique which can be used to confirm if the main fluorescence quenching of a protein occurs through a static and/or a dynamic mechanism [20]. To get a further confirmation of the involvement of a static mechanism on the association HSA:**4,** time-resolved fluorescence measurements were carried out for HSA in the absence and presence of the maximum ligand concentration used in the steady-state fluorescence experiments, at pH = 7.4. Fig. 8S in the supplementary material depicts the fluorescence decays for HSA and HSA:**4**. Serum albumin showed two fluorescence lifetimes,

with different percentage contribution, *i. e* 5.75±0.10 ns (78%) and 1.80±0.11 ns (22%) (χ^2 = 1.105), which is fully in accordance with literature results [21]. After ligand binding there was no significant change in the fluorescence lifetime for HSA: 5.71±0.10 ns (73%) and 1.75±0.11 ns (27%) (χ^2 = 1.128). Thus, since the fluorescence lifetime for HSA in the absence and presence of **4**did not change within the experimental error, it can be concluded that, in this case,the fluorescence quenching occurs through a static mechanism [22], in accordance with the ground state association HSA:**4** described above. The same behavior was previously described for other thiosemicarbazide derivatives [23,24].

Since steady-state and time-resolved fluorescence studies have shown that the fluorescence quenching of HSA is due to a static mechanism involving the formation of a non-fluorescence complex HSA:**4**, the number of binding sites (*n*) and the binding constant (K_b) at 296 K, 303 K, and 310 K can be obtained by employing a double logarithmic plot according to Eq. 2 [22]:

$$\log\left(\frac{F_0 - F}{F}\right) = \log K_b + n\log[Q] \qquad (2)$$

where F_0 and F are the steady-state fluorescence intensities of HSA in the absence and presence of **4**, respectively.

The double logarithmic plot for HSA:**4** (Fig. 9S, supplementary material) shows that *n* values were approximately 1.00 in all temperatures (Table 3), which is a clear indication that there is a single binding site for **4** on the HSA structure [25]. The K_b values are in the order of 10^4 M^{-1}, indicating a moderate interaction between HSA and **4** [19,25,26]. Thus, compound **4** can be stored and transported by this protein in the human body [23].

The interaction forces between drug and biomolecules include hydrogen bonds, van der Waals forces, electrostatic and hydrophobic interactions, which can be demonstrated from the thermodynamic parameters obtained from the van't Hoff (Eq. 3A) and Gibb's free energy equations (Eq. 3B) [27]:

$$\text{(A)} \qquad \ln K_a = -\frac{\Delta H^0}{RT} + \frac{\Delta S^0}{R} \qquad \text{(B)} \qquad \Delta G^0 = \Delta H^0 - T\Delta S^0 \qquad (3)$$

where $\Delta H°$, $\Delta S°$, and $\Delta G°$ are the enthalpy, entropy and Gibbs' free energy change, respectively. T and R are the temperature (296 K, 303 K, and 310 K) and gas constant (8.3145 $Jmol^{-1}K^{-1}$), respectively. The van't Hoff plot for HSA:**4** is shown inFig. 10S in the supplementary material and the thermodynamic parameters are given in Table 3. From the negative and positive values of $\Delta G°$ and $\Delta S°$, respectively, the binding HSA:**4** is spontaneous and entropically driven [19]. According to Ross and Subramanian proposal [28], for $\Delta H°> 0$ and $\Delta S°> 0$hydrophobic and electrostatic interactions can be suggested as the main binding forces for this interaction.

Table 3

Binding constant values (K_{SV}, k_q, n, K_b, $\Delta H°$, $\Delta S°$ and $\Delta G°$) for the interaction HSA:**4** at 296 K, 303 K, and 310 K.

Code	T (K)	K_{SV} (x10^4) (M^{-1})	k_q(x10^{12}) ($M^{-1}s^{-1}$)	n	K_b (x10^4) (M^{-1})	$\Delta H°$ ($kJmol^{-1}$)	$\Delta S°$ ($kJmol^{-1}K^{-1}$)	$\Delta G°$ ($kJmol^{-1}$)
	296	4.47±0.07	7.78	0.98±0.10	3.42±0.28			-25.7
HSA:**4**	303	4.41±0.04	7.69	1.00±0.05	4.11±0.42	17.2± 1.3	0.145± 0.004	-26.7
	310	4.12±0.03	7.16	1.01± 0.06	4.69±0.57			-27.8

Obs: r^2 for K_{SV} and k_q: 0.9981-0.9997; r^2 for n andK_b 0.9992-0.9998; r^2 for $\Delta H°$,$\Delta S°$ and $\Delta G°$ 0.9882.

2.3.2. Perturbation of the HSA structure upon ligand binding

Circular dichroism spectroscopy (CD) is a valuable technique for studying changes in the secondary structure of a protein after its interaction with small molecules. The CD spectrum for HSA at physiological pH shows negative peaks at 208 nm ($\pi \rightarrow \pi^*$ transition) and 222 nm ($n \rightarrow \pi^*$ transition), which are related to its α-helical content. The quantitative secondary structure of albumin at 208 and 222 nm can be obtained using Eq. 4 [19]:

$$\text{(A)}\ \alpha\text{-}helix\% = \frac{\left(-MRE_{208} - 4000\right)}{\left(33000 - 4000\right)}\ x\,100 \qquad \text{(B)}\ \alpha\text{-}helix\% = \frac{\left(-MRE_{222} - 2340\right)}{30300}\ x\,100 \quad (4)$$

where MRE_{208} and MRE_{222} are the mean residue ellipticity at 208 and 222 nm. The % α-helical content of the secondary structure of HSA without and in the presence of the hydrazinecarbothiamide**4** was about 68.1% and 67.7%, respectively, at 208 nm, whereas 66.7% and 65.4% at 222 nm. The quantitative decrease of 0.40% (208 nm) and 1.30% (222 nm) in the α-helical content observed in the CD results (Fig. 5A) indicatesthat there is no significant conformational change in the secondary structure of HSA upon binding of the hydrazinecarbothiamide**4** [25].

Synchronous fluorescence spectroscopy (SFS) is widely used in protein-molecule interactions to provide information about the molecular environment in the vicinity of the fluorophore groups. In SFS, a simultaneous scanning of the excitation and emission monochromators (Δλ) at 15 nm (for tyrosine) and 60 nm (for tryptophan) is performed [22]. Fig. 5B and 5C show SFS for Tyr and Trp residues for the association HSA:**4** at pH = 7.4. For both, Δλ = 15 and 60 nm, the maximum emission wavelength of Tyr and Trp residues

shows no obvious shifts, which indicates that the microenvironment around the Tyr and Trp residues is not disturbed by the presence of the hydrazinecarbothiamide**4** [22].

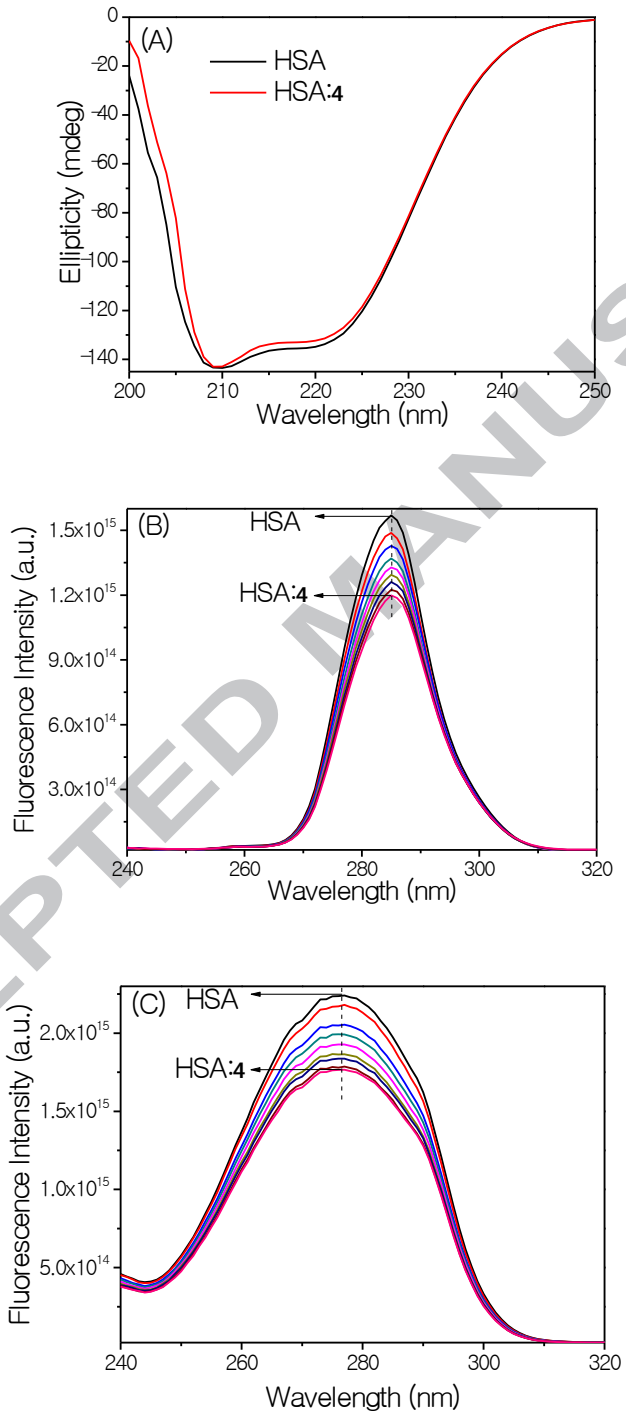

Fig. 5.(A) CD spectra of HSA in the absence and bound to **4** at pH 7.4 and 310 K. SFS for HSA without and in the presence of **4** at $\Delta\lambda$ = 15 nm (B) and $\Delta\lambda$ = 60 nm (C). [HSA] = 1.0 x 10^{-5} M and [**4**] = 0.17; 0.33; 0.50; 0.66; 0.83; 0.99; 1.15; and 1.32 x 10^{-5} M.

2.3.3. Investigation on the main binding site of 4 to HSA

HSA structure shows three major binding sites: smaller drugs mostly bind to drug sites I (also known as Sudlow's site I in subdomain IIA) or II (also known as Sudlow's site II in subdomain IIIA), while higher molecular weight ligands typically bind to site III (subdomain IB). All three sites share a common physical characteristic, *i. e*the presence of a hydrophobic pocket near multiple basic residues, which helps to explain the broad tolerance of the protein to a very diverse group of ligands. It is well known that several compounds can bind to site III of albumin; however, the number of molecules associated with sites I and II is much higher than for site III, which indicates that the former sites are of more general interest [3,29].

In this sense, competition experiments in the presence of the site markers warfarin (site I), ibuprofen (site II) and digitoxin (site III) were performed to further identify the main binding pocket for **4**. Fig. 11S in the supplementary material shows the modified Stern-Volmer plots for the association between HSA and **4** in the presence of each site marker. The calculated binding constants (K_b) in the presence of warfarin, ibuprofen, and digitoxin were $(2.63\pm0.20)\text{x}10^4$, $(3.63\pm0.17)\text{x}10^4$, and $(4.40\pm0.19)\text{x}10^4$ M^{-1}, respectively. Since the K_b value has changed significantly only in the presence of warfarin (43.9%), this is a clear indication that the main binding site for hydrazinecarbothiamide**4** is subdomain IIA, Sudlow's site I [3,7],the exact site where the Trp-214 residue can be found

In order to identify the main amino acid residues as well as the main binding forces involved in the association HSA:**4**, molecular docking calculations were carried out. Fig. 6 depicts the main amino acid residues that are able to interact with the ligand inside the protein binding site.

Molecular docking results also suggested hydrophobic and electrostatic interactions as the main binding forces, which is in accord to the experimental data.Additionally, hydrogen bonding was also detected by theoretical calculations. The N-H group of the indole moiety of Trp-214 is a potential hydrogen bond donor to one of the nitrogen atoms of the ligand structure, within a distance of 2.40 Å, while the carboxylate group of Glu-449 is ahydrogen bond acceptor fromone of the N-H groups of the ligand, within a distance of 2.00 Å. Molecular docking also suggests an electrostatic interaction between the bromine group of the ligand with the $–NH_3^+$group from Lys-198 residue, within a distance of 2.30 Å. Finally, hydrophobic interactions occur between the thiosemicarbazide **4** and Leu-452 and Leu-480 residues.

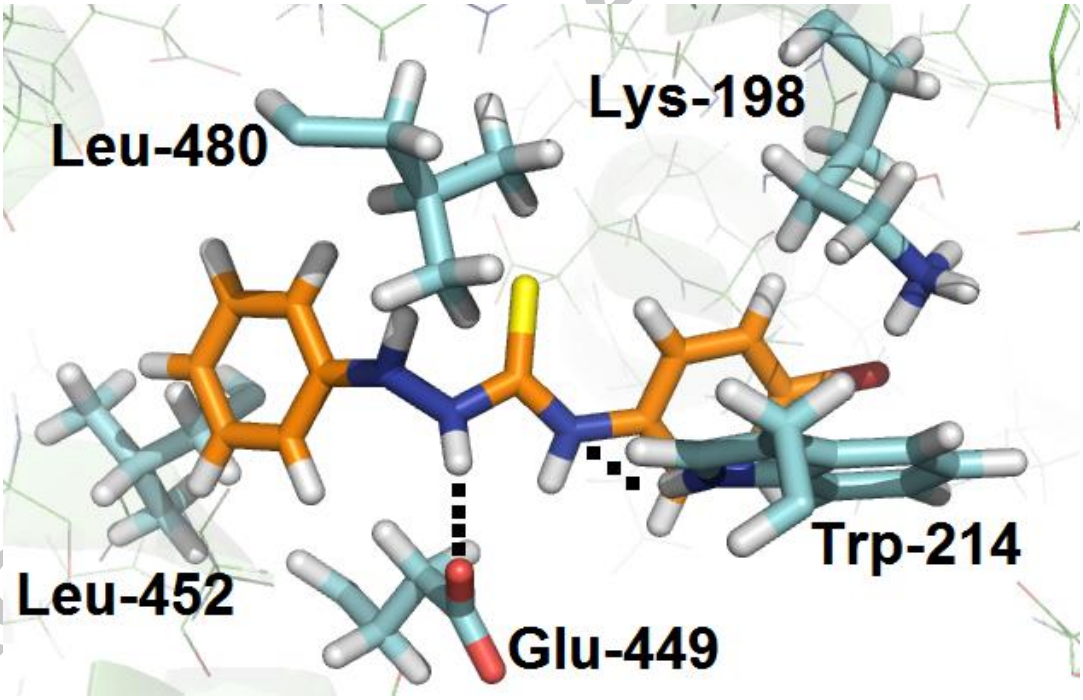

Fig. 6. Best score poses for the interaction HSA:**4** inside Sudlow's site I (*ChemPLP* function). Select amino acid residues and hydrazinecarbothiamide **4**carbon atoms are represented in cyan and orange, respectively. Black dots represent interaction *via* hydrogen bonding. Hydrogen: white; oxygen: red; bromine: brownish red; sulfur: yellow and nitrogen: dark blue.

3. Conclusion

In summary, six hydrazinecarbothiamides were prepared using two known synthetic methods and a novel method employing a solvent-free grinding. The later method strictly follows the principles of Green Chemistry. The mechanochemical grinding under solvent-free conditions resulted in quantitative yields, higher purity and in lower reaction time compared to the conventional and microwave-assisted methods. Hydrazinecarbothiamide**4** showed the best tyrosinase inhibition (IC_{50} = 22.6 µM), even better than the usual standard, *i. e* commercial ascorbic acid (IC_{50} = 266 µM). The inhibition mechanism of tyrosinase is uncompetitive, therefore there is the formation of a ternary complex enzyme-substrate-inhibitor (ESI). Molecular docking results suggest *t*-Stacking interaction as a critical force between the two better tyrosinase inhibitors, *i. e***3** and **4**, and the substrate L-DOPA. Finally, molecular docking results also suggested that the hydrazinecarbothiamide**4** can interact with the amino acid residuesAla-79, His-243, Val-247, Phe-263, Val-282, and Glu-321 *via* hydrogen bonding and hydrophobic forces. For the interaction HSA:**4**, the main fluorescence quenching mechanism is *via* a static process, which results in a ground-state association. The binding is spontaneous, moderate and entropically driven. The interaction does not perturb significantly the secondary structure of the albumin as well as the microenvironment around the Trp and Tyr residues. Competitive experiments indicated that Sudows's site I is the HSA main binding site for compound **4** and molecular docking results suggest hydrogen bonding, hydrophobic and electrostatic interactions as the main binding forces between the ligand **4** and amino acid residues Lys-198, Trp-214, Glu-449, Leu-452, and Leu-480. Overall, in addition to the fact that hydrazinecarbothiamide**4** presented the best tyrosinase inhibition, it can be easily transported and distributed by HSA in the human bloodstream.

4. Experimental

4.1. General information

The melting points of the products were determined on a Meltemp II apparatus and were not corrected. Nuclear magnetic resonance (^{1}H- and DEPTQ-NMR) spectra were recorded on a Bruker Avance III spectrometer (^{1}H, 500 MHz; DEPT Q, 125 MHz) using tetramethylsilane (TMS) as the internal standard and acetone-d_6 or DMSO-d_6 as the solvent. Infrared spectra (KBr pellets) were recorded on a Bruker Vertex 70 spectrophotometer. Elemental analyses were performed on a Perkin-Elmer Model 2400 instrument. The microwave-assisted organic reactions were performed in a CEM Discovery System reactor.

Commercially available phenylhydrazine, 4-X-phenyl-isothiocyanates, tyrosinase from mushroom lyophilized enzyme, (*S*)-2-amino-3-(3,4-dihydroxyphenyl)-propanoic acid (L-DOPA), 2,2',2",2"'-(ethane-1,2-diylbis(azanetriyl))-tetraacetic acid (EDTA), ascorbic acid, dimethyl sulfoxide (DMSO, spectroscopic grade), HSA, warfarin, ibuprofen, digitoxin and PBS buffer were purchased from Sigma-Aldrich Chemical Company. Methanol (spectroscopic grade) and toluene were obtained from Tedia Ltd. One tablet of commercial PBS dissolved in 200 mL of Milli-Q water yields 1.00 x 10^{-2} M phosphate buffer, 2.70 x 10^{-3} M potassium chloride and 1.37 x 10^{-1} M sodium chloride.

4.2. General procedure for the synthesis of hydrazinecarbothiamides (1-6)

Hydrazinecarbothiamides**1-6** were obtained by an anhydrous acylation reaction between phenylhydrazine and 4-X-phenyl-isothiocyanates through three different methods. All hydrazinecarbothiamides were identified by melting point, FT-IR, NMR data and elemental analyses [11,12].

*Method I:*Under Magnetic Stirring

The different aryl isothiocyanates (25 mmol) and phenylhydrazine (25 mmol) were mixed in the presence of boiling toluene (20 mL). The reaction mixture was stirred for 60 minutes at room temperature and was monitored by TLC. The solid product was obtained by filtration, washed with ice-cold toluene and recrystallized from ethanol [11].

*Method II:*Under Microwave Irradiation

The mixture containing the aryl isothiocyanate (25 mmol) and phenylhydrazine (25 mmol) was submitted to microwave irradiation for 30 min at 100 W, in the presence of toluene. The completion of the reaction was monitored by TLC. The solid obtained was filtered and washed with ice-cold toluene. The hydrazinecarbothiamides were recrystallized from ethanol [11].

*Method III:*Under solvent-free grinding

The aryl isothiocyanates (0.74 mmol) and phenylhydrazine (0.74 mmol) were mixed for 2 minutes in a porcelain mortar and pestle in the absence of any organic solvent, at room temperature (monitored by TLC). The solid formed was obtained in high purity without recrystallization.

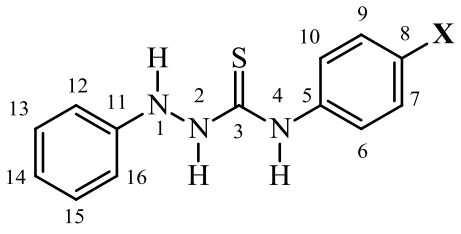

(**1**) **X** = H
(**2**) **X** = NO_2
(**3**) **X** = Cl
(**4**) **X** = Br
(**5**) **X** = OCH_3
(**6**) **X** = CH_3

4.2.1. N-2-diphenylhydrazinecarbothioamide(**1**).White solid; m.p 173-171 °C; FT-IR (KBr, υ cm^{-1}): 3282, 3212, 3170 (N-H), 1594, 1542, 1496 (C=C), 1207 (C=S);^{1}H NMR (500 MHz, acetone-d^6) δ 9.66 (s, 1H, H-2), 8.70 (s, 1H, H-4), 7.73 (d, 2H, *J* = 7.78 Hz,H-6, H-10), 7.42 (s, 1H, H-1), 7.29 (t, 2H,*J* = 7.78 Hz,H-7, H-9), 7.25 (t, 2H, *J* = 7.78 Hz,

H-13, H-15), 7.12 (t, 1H, *J* = 7.28 Hz, H-8), 6.89 (t, 1H, *J* = 7.28 Hz, H-14), 6.87 (d, 2H, *J* = 7.78 Hz, H-12, H-16). DEPT Q NMR (125 MHz, acetone-d_6) δ 183.2 (C-3), 149.0 (C-11), 140.5 (C-5), 130.3 (C-13, C-15), 129.2 (C-7, C-9), 126.0 (C-8), 125.2 (C-6, C-10), 122.0 (C-14), 114.6 (C-12, C-16). Anal. calcd for $C_{13}H_{13}N_3S$: C, 64.17; H, 5.39; N, 17.27. Found: C, 64.22; H, 5.40; N, 17.23.

4.2.2. N-(4-nitrophenyl)-2-phenylhydrazinecarbothioamide (**2**)**.**Yellowsolid; m.p 234-233 °C; FT-IR (KBr, υ cm^{-1}): 3435, 3249, 3190 (N-H), 1600, 1568, 1504 (C=C), 1280 (C=S), 1504 (C-NO_2); ^{1}H NMR (500 MHz, acetone-d^6) δ 10.19 (s, 1H, H-2), 9.08 (s, 1H, H-4), 8.20 (t, 2H,*J* = 8.47 Hz,H-13, H-15), 8.20 (d, 2H, H-7, H-9), 7.50 (s, 1H, H-1), 7.27 (t, 2H, *J* = 8.47 Hz, H-12, H-16), 6.89 (d, 2H, *J* = 9.60 Hz, H-6, H-10), 6.91 (t, 1H,*J* = 5.65 Hz, H-14); DEPT Q NMR (125 MHz, acetone-d_6) δ 183.0 (C-3), 148,8 (C-11), 146.8 (C-5), 145.1 (C-8), 130.5 (C-13, C-15), 125.0 (C-7, C-9), 124.1 (C-6, C-10), 122.5 (C-14), 114.9 (C-12, C-16). Anal. calcd for $C_{13}H_{12}N_4O_2S$: C, 54.16; H, 4.20; N, 19.43. Found: C, 54.12; H, 4.25; N, 19.38.

4.2.3. N-(4-chlorophenyl)-2-phenylhydrazinecarbothioamide (**3**).White solid; m.p 234-233 °C; FT-IR (KBr, υ cm^{-1}): 3435, 3315, 3140 (N-H), 1600, 1554, 1508 (C=C), 1286 (C=S), 1209, 758 (C-Cl); ^{1}H NMR (500 MHz, acetone-d^6) δ 9.79 (s, 1H, H-2), 8.85 (s, 1H, H-4), 7.77 (d, 2H, *J* = 8.51 Hz, H-7, H-9), 7.45 (s, 1H, H-1), 7.31 (d, 2H, *J* = 8.51 Hz, H-6, H-10), 7.25 (t, 2H, *J* = 7.72 Hz, H-13, H-15), 6.89 (t, 1H, *J* = 7.25 Hz, H-14), 6.88 (d, 2H, *J* = 7.88 Hz, H-12, H-16); DEPT Q NMR (125 MHz, *acetone*-d_6) δ 183.2 (C-3), 148.9 (C-11), 139.3 (C-5), 130.5 (C-8), 130.2 (C-13, C-15), 129.1 (C-7, C-9), 126.8 (C-6, C-10), 121.8 (C-14), 114.5 (C-12, C-16). Anal. calcd for $C_{13}H_{12}ClN_3S$: C, 56.21; H, 4.35; N, 15.13. Found: C, 56.19; H, 4.39; N, 15.08.

4.2.4. N-(4-bromophenyl)-2-phenylhydrazinecarbothioamide (**4**). White solid; m.p 212-209 °C; FT-IR (KBr, υ cm^{-1}): 3249, 3182 (N-H), 1597, 1585, 1489 (C=C), 1199 (C=S), 1072, 769 (C-Br); ^{1}H NMR (500 MHz, acetone-d^6) δ 9.81 (s, 1H, H-2), 8.85 (s, 1H, H-4), 7.74 (d, 3H, *J* = 8.20 Hz, H-7, H-9), 7.46 (s, 1H, H-1), 7.46 (t, 2H, *J* = 8.51 Hz,H-6, H-10), 7.24 (t, 3H,*J* = 7.57 Hz, H-13, H-15), 6.90 (t, 1H, H-14), 6.87 (d, 2H, *J* = 7.57 Hz, H-12, H-16); ^{13}C NMR (125 MHz, DMSO-d_6) δ 181.1 (C-3), 147.9 (C-11), 138.7 (C-5), 130.7 (C-7, C-9),

128.9 (C-13, C-15), 127.2 (C-6, C-10), 119.9 (C-14), 116.9 (C-8), 113.1 (C-12, C-16). Anal. calcd for $C_{13}H_{12}BrN_3S$: C, 48.46; H, 3.75; N, 13.04. Found: C, 48.42; H, 3.81; N, 12.98.

4.2.5. N-(4-methoxyphenyl)-2-phenylhydrazinecarbothioamide (**5**).White solid; m.p. 186-184 °C; IR (KBr, υ cm^{-1}): 3267, 3161, 3091 (N-H), 3028 (C-H), 1600, 1548, 1492 (C=C), 1247 (C=S), 1170 (ArC-O), 1026 (Ar-O-C); ^{1}H NMR (500 MHz, acetone-d_6) δ 9.51 (s, 1H, H-2), 8.60 (s, 1H, H-4), 7.53 (d, 2H, *J* = 9.64 Hz, H-12, H-16), 7.38 (s, 1H, H-1), 7.25 (t, 2H, *J* = 9.64 Hz, H-13, H-15), 6.88 – 6.84 (m, 5H, H-6, H-7, H-9, H-10, H-14), 3.76 (s, 3H, OCH_3); DEPT Q NMR (125 MHz, acetone-d^6) δ 183.6 (C-3), 158.5 (C-8), 149.2 (C-11), 133.4 (C-5), 130.3 (C-13, C-15), 127.4 (C-6, C-10), 121.9 (C-14), 114.6 (C-12, C-16), 114.4 (C-7, C-9), 56.0 (OCH_3). Anal. calcd for $C_{14}H_{15}N_3OS$: C, 61.52; H, 5.53; N, 15.37. Found: C, 61.57; H, 5.48; N, 15.43.

4.2.6. N-(p-tolyl)-2-phenyl-hydrazinecarbothioamide (**6**).White solid; m.p 175-174 °C; IR (KBr, υ cm^{-1}): 3437, 3275, 3186 (N-H), 3020 (C-H), 1627, 1550, 1490 (C=C), 1269 (C=S); ^{1}H NMR (500 MHz, acetone-d^6) δ 9.57 (s, 1H, H-2), 8.63 (s, 1H, H-4), 7.57 (d, 2H, *J* = 8.03 Hz, H-6, H-10), 7.38 (s, 1H, H-1), 7.25 (t, 2H, *J* = 7.78 Hz, H-13, H-15), 7.09 (d, 2H,*J* = 7.78 Hz, H-7, H-9), 6.88 (t, 1H, *J* = 7.46 Hz,H-14), 6.88 (d, 2H, *J* = 7.53 Hz, H-12, H-16), 2.28 (s, 3H; CH_3); DEPT Q NMR (125 MHz, acetone-d_6) δ 182.9 (C-3), 148.7 (C-11), 137.5 (C-5), 135.2 (C-8), 129.9 (C-13, C-15), 129.4 (C-7, C-9), 125.0 (C-6, C-10), 121.6 (C-14), 114.2 (C-12, C-16), 20.8 (CH_3). Anal. calcd for $C_{14}H_{15}N_3S$: C, 65.34; H, 5.87; N, 16.33. Found: C, 64.39; H, 5.83; N, 16.28.

4.3. Tyrosinase inhibition assays

4.3.1. Experimental assays

The UV-Vis absorption spectrum for tyrosinase in the activity measurements was recorded on a Shimadzu UV-Vis spectrophotometer UV Mini 1240 (Kyoto, Japan), at room temperature. Tyrosinase inhibition activity was measured by the method of Amorim *et.al.*[30] Firstly, stock solutions of hydrazinecarbothiamide derivatives**1**-**6** (2.50 mM) were prepared by dissolving them in DMSO. Then, each thiosemicarbazide was mixed with L-DOPA (0.17 mM), EDTA (0.022 mM) and tyrosinase (50–100 units), in PBS (pH=7.4). Due to the fact

thatthe hydrazinecarbothiamidesshowed different solubility in water, the concentration of the compounds **1**-**6** used to determine the % inhibition was 666; 466; 333; 66.6; 167; and 167 µM, respectively. When the tyrosinase solution was added to the mixture, the absorbance was immediately measured at 475 nm and the formation of L-Dopaquinone was monitored for 30 min (Scheme 2) [31].

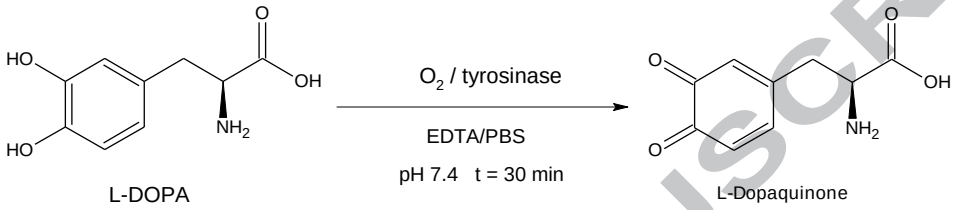

Scheme 2. Oxidation of L-DOPA to L-Dopaquinone by tyrosinase enzyme.

The inhibition percentage was calculated according to the following equation (Eq. 5) [31]:

$$Inhibition\ \% = \frac{[(B_{30} - B_0) - (A_{30} - A_0)]}{(B_{30} - B_0)} x\ 100 \quad (5)$$

where B_0 and B_{30} are the absorbance of L-DOPA + tyrosinase at t = 0 min and t = 30 min, respectively. A_0 and A_{30} are the absorbance of L-DOPA + tyrosinase + inhibitor at t = 0 min and t = 30 min, respectively. In Eq. 1, the possible interference of the absorbance of organic compounds was subtracted.

The IC_{50} value for the hydrazinecarbothiamides**1**, **2**, **3** and **4** was calculated from the equation generated by a polynomial fit of the experimental data (Origin software, ANOVA statistical function). Commercial ascorbic acid (IC_{50} = 266 µM) was used as a positive control [32]. The final inhibitor concentration to each assay which was used to calculate the IC_{50} value was 66.66; 133; 200; 400; 533; and 667 µM.

The inhibitory mechanism of oxidation of L-DOPA on mushroom tyrosinase when in presence of hydrazinecarbothiamides**3** and **4** (the two most promising tyrosinase inhibitors) was determined from Hanes-Woolf plots. In this analysis, different concentrations of L-DOPA (66.6; 100; 200; 333; 467; and 667 μM) as substrate and different concentrations ofhydrazinecarbothiamides**3** and **4** (0; 33.3; 50.0; and 83.0 μM). L-Dopaquinone production was analyzed in the absence and presence of the inhibitors after incubation for 30 min at 310 K and the absorbance was measured at 475 nm.

4.4. Spectroscopic analysis of the interaction between HSA and hydrazinecarbothiamide 4

UV-vis and steady-state fluorescence spectra were measured on a Jasco J-815 spectropolarimeter using a quartz cell (1.0 cm optical path) equipped with a Peltier thermal-controlled cuvette holder Jasco PFD-425S15F. UV-vis spectrum of **4** (1.32×10^{-5} M, in PBS) was measured in the 200-400 nm range at 310 K.Since, both HSA and hydrazinecarbothiamide**4** showed UV absorption in the 200-300 nm range(Fig. 12S in the supplementary material), the effect probably observed on the UV-Vis absorption spectrum of HSA upon ligand addition will be due to the contribution of the ligand absorption and not due to ligand-protein complex formation. For this reason, other spectroscopic techniques were employed, such as circular dichroism, steady state, time-resolved and synchronous fluorescence to explore the structural change of protein and ligand-protein complex.

In order to compensate the inner filter effect, the steady-state fluorescence intensity for HSA:**4**was corrected by the absorption of the ligand at excitation (λ = 280 nm) and emission (λ = 340 nm) wavelengths (Fig. 12S in the supplementary material), using Eq. 6 [33]:

$$F_{cor} = F_{obs} 10^{[(A_{ex} + A_{em})/2]} \quad (6)$$

where F_{cor} and F_{obs} are the corrected and the observed fluorescence intensity values, respectively. A_{ex} is the experimental absorbance value at the excitation wavelength in PBS (280 nm, ε = 7845 $M^{-1}cm^{-1}$). A_{em} is the experimental absorbance value at the emission wavelength in PBS (340 nm, ε = 1454 $M^{-1}cm^{-1}$).

Steady-state fluorescence spectra were collected in the 290-450 nm range at 296 K, 303 K and 310 K, with λ_{exc} = 280 nm. Using a microliter syringe, successive aliquots of a stock solution of **4** were added to a 3.0 mL solution of HSA (1.00 x 10^{-5} M, at pH = 7.4), leading to final ligand concentrations of 0.17; 0.33; 0.50; 0.66; 0.83; 0.99; 1.15; and 1.32 x 10^{-5} M.

Competitive binding studies were carried out using the HSA site markers warfarin, ibuprofen and digitoxin. The proportion between HSA and each site marker was 1:1 (1.00 x 10^{-5} M concentration, at pH = 7.4). Using a microliter syringe, successive aliquots of a stock solution of hydrazinecarbothiamide**4** were added to a 3.0 mL solution of HSA:site marker, at 310 K. The final ligand concentration after each addition was the same as described above.

Time-resolved fluorescence measurements were performed on an Edinburgh Instruments fluorimeter model FL920 CD, equipped with an EPL laser (excitation wavelength of 280 ± 10 nm; pulse width of 850 ps; energy per pulse of 1.8 μW). The fluorescence decay of a 1.0 x 10^{-5} M solution of HSA (3.0 mL at pH = 7.4) was monitored at 340 nm in the absence and presence of the maximum concentration of the ligand used in the steady-state fluorescence studies (1.32 x 10^{-5} M). The fluorescence decay lifetime for HSA and HSA:**4** was analyzed using the deconvolution software of the fluorimeter.

Synchronous fluorescence spectra (SFS) were performed in an Edinburgh Instruments fluorimeter model Xe900. SFS were obtained by setting Δλ = 15 nm and 60 nm, for tyrosine

and tryptophan residues, respectively, at room temperature. Using a microliter syringe, successive aliquots of a stock solution of hydrazinecarbothiamide**4** were added to a 3.0 mL solution of HSA. The final ligand concentrations were the same to those employed in the steady-state fluorescence studies.

Circular dichroism (CD) spectra were recorded from 250 to 200 nm on a Jasco J-815 spectropolarimeter, equipped with a Peltier thermal-controlled cuvette holder. The spectra of a 1.00 x 10^{-5} M solution of HSA were recorded in the absence and in the presence of the maximum ligand concentration used in the steady-state fluorescence studies (1.32 x 10^{-5} M), at 310 K. The spectra were collected and averaged over three scans. The CD signal reported as ellipticity (in millidegrees) can be converted in mean residue ellipticity: $[\theta]MRW = \theta_{obs}(0.1MRW)/(cl)$ (in deg cm^2 $dmol^{-1}$), where θ_{obs} is the observed ellipticity in millidegrees, MRW is the protein mean weight (molecular weight of the protein in daltons/number of residues), *c* is the concentration in milligrams per milliliter, and *l* is the length of the light path in centimeters.

4.5. Molecular docking analysis for tyrosinase and HSA

The chemical structure of the hydrazinecarbothiamides under study, *i. e***1-6**, and L-DOPA were built and energy-minimized by Density Functional Theory (DFT) calculations (B3LYP potential) with basis set 6-31G*, available in the Spartan'14 program.

The molecular docking studies were performed with the GOLD 5.2 program (CCDC, *Cambridge Crystallographic Data Centre*) and the crystallographic structure of tyrosinase and HSA were obtained from Protein Data Bank, with access code 2Y9X [34] and 1N5U [10], respectively. Hydrogen atoms were added to each protein structure according to the data inferred by GOLD 5.2 program on the ionization and tautomeric states. For tyrosinase, a 10 Å radius spherical cavity around the dicopper center was defined as the binding site for the

molecular docking calculations. On the other hand, for HSA molecular docking interaction cavity in the protein was established with a 10 Å radius from the Trp-214 residue. The scoring function used was '*GoldScore*' and '*ChemPLP*', for tyrosinase and HSA, respectively. For furtherinformationseepreviouspublications [8,32,35].

Acknowledgments

This research was supported by the Brazilian funding agencies: Coordenação de Aperfeiçoamento de Pessoal de Nível Superior (CAPES), Conselho Nacional de Desenvolvimento Científico e Tecnológico (CNPq) and Fundação de Amparo à Pesquisa do Estado do Rio de Janeiro (FAPERJ). The authors also acknowledge Prof. Dr. Nanci Camara de Lucas Garden (Chemistry Institute - UFRJ) for the time-resolved and synchronous fluorescence facilities.

References

[1]Y. Wang, M.-M. Hao, Y. Sun, L.-F. Wang, H. Wang, Y.-J. Zhang, H.-Y. Li,P.-W. Zhuang, Z. Yang, Synergistic promotion on tyrosinase inhibition by antioxidants, Molecules23 (2018) 106-118.

[2]N. Gençer, D. Demir, F. Sonmez, M. Kucukislamoglu, New saccharin derivatives as tyrosinase inhibitors,Bioorg. Med. Chem. 20 (2012) 2811–2821.

[3]O.A. Chaves, M.R.L. Santos, M.C.C. de Oliveira, C.M.R. Sant'Anna, R.C. Ferreira, A. Echevarria, J.C. Netto-Ferreira, Synthesis, tyrosinase inhibition and transportation behavior of novel β-enamino thiosemicarbazide derivatives by human serum albumin, J. Mol. Liq. 254 (2018) 280-290.

[4]J. Liu, W. Yi, Y. Wan, L. Ma, H. Song, 1-(1-Arylethylidene) thiosemicarbazide derivatives: A new class of tyrosinase inhibitors,Bioorg. Med. Chem. 16 (2008) 1096-1102.

[5]J. Liu, C. Chen, F. Wu, L. Zhao, Microwave-assisted synthesis and tyrosinase inhibitory activity of chalcone derivatives, Chem. Biol. Drug Des. 82 (2013) 39–47.

[6]I. Strelec, P. Burić, I. Janković, T. Kovač, M. Molnar, Inhibitory effect of coumarin derivatives on apple (cv. Idared) polyphenol oxidase. Croat. J. Food Sci. Technol. 9 (2017) 57-65.

[7]A.S. Abdelhameed, A.H. Bakheit, F.M. Almutairi, H. AlRabiah, A.A. Kadi, Biophysical and in silico studies of the interaction between the anti-viral agents acyclovir and penciclovir, and human serum albumin, Molecules 22 (2017) 1906-1920.

[8]O.A. Chaves, A.P.O. Amorim, L.H.E. Castro, C.M.R. Sant'Anna, M.C.C. de Oliveira, D. Cesarin-Sobrinho, J.C. Netto-Ferreira, A.B.B. Ferreira, Fluorescence and docking studies of the interaction between human serum albumin and pheophytin, Molecules 20 (2015) 19526-19539.

[9]A. Szkudlarek, D. Pentak, A. Ploch, J. Pozycka, M. Maciazek-Jurczyk,*In vitro* investigation of the interaction of tolbutamide and losartan with human serum albumin in hyperglycemic states, Molecules 22 (2017) 2249-2277.

[10]M. Wardell, Z. Wang, J.X. Ho, J. Robert, F. Ruker, J. Ruble, D.C.Carter, The atomic structure of human methemalbumin at 1.9 Å,Biochem. Biophys. Res. Commun,291 (2002) 813–819.

[11]C.M. dos Reis, D. Sousa-Pereira, R.O. Paiva, L.F. Kneipp, A. Echevarria,Microwave-assistedsynthesisofnew N_1,N_4-substituted thiosemicarbazones,Molecules16 (2011) 10668-10684.

[12]A.F.M. Fahmy, A.A. El-Sayed, M.M. Hemdan, A.I. Hassaballah, A.F. Mabied, Synthesis of N-containing heterocycles via mechanochemical grinding and conventional techniques, Asian J. Chem. 29 (2017) 2679-2686.

[13]M. Gupta, S. Paul, R. Gupta, General aspects of 12 basic principles of green chemistry with applications,Curr. Sci. 99 (2010) 1341-1360.

[14]M.M. Britto, T.M.G. Almeida, A. Leitão, C.L. Donnici, M.T.P. Lopes, C.A. Montanari, Synthesis of mesoionic 4-(para-substituted phenyl-5-2,4-dichlorophenyl)-1,3-4-thiadiazolium-2-amidines by direct cyclization via acylation of thiosemicarbazides,Synth. Comm. 36 (2006) 3359-3369.

[15]S. Begum, M.I. Choudhary, K.M. Khan, Synthesis, phytotoxic, cytotoxic, acetylcholinesterase and butrylcholinesterase activities of N,N'-diaryl unsymmetrically substituted thioureas, Nat. Prod. Res. 23 (2009) 1719-1730.

[16]L. Zhang, J.-J. Chang, S.-L. Zhang, G.L.V. Damu, R.-X. Geng, C.-H.Zhou, Synthesis and bioactive evaluation of novel hybrids of metronidazole and berberine as new type of antimicrobial agents and their transportation behavior by human serum albumin,Bioorganic. Med. Chem. 21 (2013) 4158–4169.

[17]L. Naso, V.R. Martínez, L. Lezama, C. Salado, M. Valcarcel, E.G. Ferrer, P.A.M.Williams, Antioxidant, anticancer activities and mechanistic studies of the flavone glycoside diosmin and its oxovanadium(IV) complex. Interactions with bovine serum albumin,Bioorg Med Chem. 24 (2016) 4108–4119.

[18]M. Montalti, A. Credi, L. Prodi, M.T. Gandolfi,Handbook of Photochemistry. 3rd ed. CRC Press, Taylor & Francis; 2006.

[19]O.A. Chaves, Mathew B, D. Cesarin-Sobrinho, B. Lakshminarayanan, M. Joy, G.E. Mathew, J. Suresh, J.C. Netto-Ferreira, Spectroscopic, zeta potential and molecular docking analysis on the interaction between human serum albumin and halogenated thienyl chalcones, J. Mol. Liq. 242 (2017) 1018-1026.

[20]J. R.Lakowicz, Principles of Fluorescence Spectroscopy, 3rd ed.; Springer: New York, 2006.

[21]H. Sun, Y. Liu, M. Li, S. Han, X. Yang, R. Liu, Toxic effects of chrysoidine on human serumalbumin: isothermal titration calorimetry and spectroscopic investigations,Luminescence 31 (2016) 335-340.

[22]O.A. Chaves, D. Cesarin-Sobrinho, C.M.R. Sant'Anna, M.G. de Carvalho, L.R. Suzart, F.E.A. Catunda-Junior, J.C. Netto-Ferreira, A.B.B. Ferreira, Probing the interaction between 7-O-β-d-glucopyranosyl-6-(3-methylbut-2-enyl)-5,4-dihydroxyflavonol with bovine serum albumin (BSA), J.Photochem.Photobiol. A. 336 (2017) 32-41.

[23]F.-L. Cui, J. Fan, J.-P. Li, Z.-D. Hu,Interactions between 1-benzoyl-4-p-chlorophenyl thiosemicarbazide and serum albumin: investigation by fluorescence spectroscopy,Bioorg. Med. Chem. 12 (2004) 151-157.

[24]M. Lomzik, M. Brindell, Synthesis and interaction with albumin of N,N-dimethylaminbenzyl derivative of thiosemicarbazone and its ruthenium(II) complex,CHEMIK. 67 (2013) 91-98.

[25]O.A. Chaves, B.A. Soares, M.A.M. Maciel, C.M.R. Sant'Anna, J.C. Netto-Ferreira, D. Cesarin-Sobrinho, A.B.B. Ferreira,A Study of the interaction between trans-dehydrocrotonin, a bioactive natural 19-nor-clerodane, and serum albumin, J Braz Chem Soc. 27 (2016) 1858-1865.

[26]J. Ruiz, C. Vicente, C. de Haro, D. Bautista, Novel bis-C,N-cyclometalated iridium(III) thiosemicarbazide antitumor complexes: interactions with human serum albumin and DNA, and inhibition of cathepsin B,Inorg. Chem. 52 (2013) 974–982.

[27]Q. Wang, X. Liu, M. Su, Z. Shi, H. Sun, Study on the interaction characteristics of cefamandole with bovine serum albumin by spectroscopic technique,Spectrochim. Acta A Mol. Biomol. 136 (2015) 321–326.

[28]P.D. Ross, S. Subramanian, Thermodynamics of protein association reactions: forces contributing to stability, Biochemistry 20 (1981) 3096-3102.

[29]B. Zhao, J. Sensintaffar, Z. Bian, J. Belmar, T. Lee, E.T. Olejniczak, S.W.Fesik, Structure of a myeloid cell leukemia-1 (Mcl-1) inhibitor bound to drug site 3 of human serum albumin,Bioorg. Med. Chem. 25 (2017) 3087–3092.

[30]A.P.O. Amorim, M.C.C. de Oiveira, T.A. Amorim, A. Echevarria, Antioxidant, iron chelating and tyrosinase inhibitory activities of extracts from *Talinum triangulare Leach*stem,Antioxidants2 (2013) 90-99.

[31]O.A. Chaves, L.S. Barros, M.C.C. de Oliveira, C.M.R. Sant'Anna, A.B.B. Ferreira, F.A. da Silva, D. Cesarin-Sobrinho, J.C. Netto-Ferreira,Biological interactions of fluorinated chalcones: Stimulation of tyrosinase activity and binding to bovine serum albumin,J. Fluor. Chem. 199 (2017) 30–38.

[32]M.A. Soares, M.A. Almeida, C. Marins-Goulart, O.A. Chaves, A. Echevarria, M.C.C. de Oliveira,Thiosemicarbazones as inhibitorsoftyrosinaseenzyme,Bioorganic Med. Chem. 27 (2017) 3546–3550.

[33]O.A. Chaves, C.S.H. Jesus, P.F. Cruz, C.M.R. Sant'Anna, R.M.M. Brito, C. Serpa, Evaluation by fluorescence, STD-NMR, docking and semi-empirical calculations of the o-NBA photo-acid interaction with BSA,Spectrochim. Acta A Mol. Biomol. Spectrosc. 169 (2016) 175–181.

[34]W.T. Ismaya, H.J. Rozeboom, A. Weijn, J.J. Mes, F. Fusetti, H.J. Wichers, B.W. Dijkstra, Crystal structure of *AgaricusBisporus*mushroom tyrosinase: Identity of the tetramer subunits and interaction with tropolone, Biochemistry 50 (2011) 5477-5486.

[35]O.A. Chaves, C.H.C.S. de Oliveira, R.C. Ferreira, R.P. Pereira, J.L.R. de Melos, C.E. Rodrigues-Santos, A. Echevarria, D. Cesarin-Sobrinho, Investigation of interaction between human plasmatic albumin and potential fluorinated anti-trypanosomal drugs, J. Fluor. Chem. 199 (2017) 103-112.

Graphical abstract

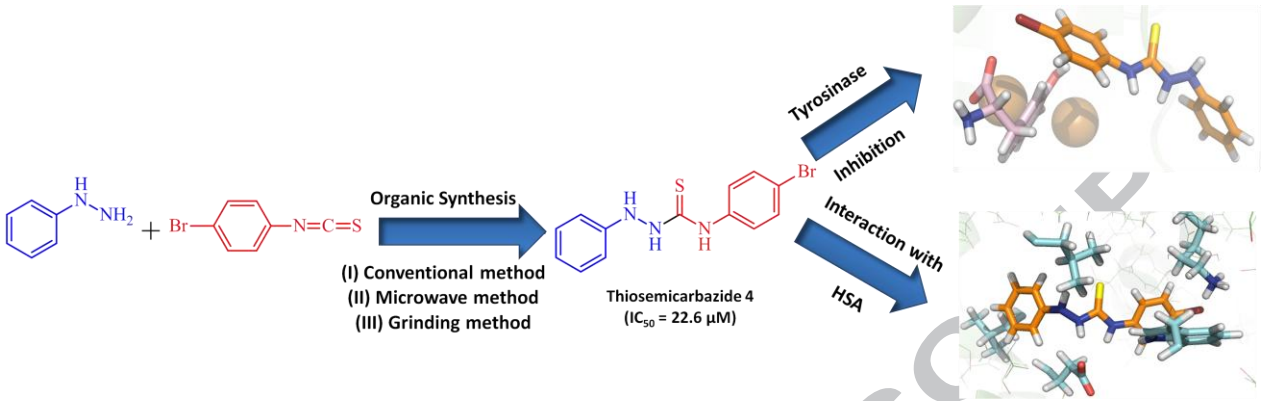

Highlights

*A series of hydrazinecarbothioamide derivatives were synthesized *via* conventional, microwave and grinding methods.

*Hydrazinecarbothioamide **4**, showed the best tyrosinase inhibition (IC_{50} = 22.6 µM) with an uncompetitive mechanism.

*Molecular docking suggested that **4** interacts *via* hydrogen bonding and hydrophobic forces with tyrosinase.

*Interaction HSA:**4** is spontaneous, entropically driven, moderate and occurs inside Sudlow's site I (subdomain IIA).